Title

Structural connections of the centromedian nucleus of thalamus and their relevance for neuromodulation in generalized drug-resistant epilepsy: insight from a tractography study.

Permalink

Authors

Remore, Luigi

Rifi, Ziad

Nariai, Hiroki

et al.

Publication Date

2023

DOI

Peer reviewed

Structural connections of the centromedian nucleus of thalamus and their relevance for neuromodulation in generalized drug-resistant epilepsy: insight from a tractography study

Luigi G. Remore [ID], **Ziad Rifi, Hiroki Nariai, Dawn S. Eliashiv, Aria Fallah, Benjamin D. Edmonds, Joyce H. Matsumoto, Noriko Salamon, Meskerem Tolossa, Wexin Wei, Marco Locatelli, Evangelia C. Tsolaki* and Ausaf A. Bari***

Abstract

Background: Epilepsy is a widespread neurologic disorder and almost one-third of patients suffer from drug-resistant epilepsy (DRE). Neuromodulation targeting the centromediannucleus of the thalamus (CM) has been showing promising results for patients with generalized DRE who are not surgical candidates. Recently, the effect of CM- deep brain stimulation (DBS) in DRE patients was investigated in the Electrical Stimulation of Thalamus for Epilepsy of Lennox–Gastaut phenotype (ESTEL) trial, a monocentric randomized-controlled study. The same authors described a 'cold-spot' and a 'sweet-spot', which are defined as the volume of stimulation in the thalamus yielding the least and the best clinical response, respectively. However, it remains unclear which structural connections may contribute to the anti-seizure effect of the stimulation.
Objective: We investigated the differences in structural connectivity among CM, the sweet-spot and the cold-spot. Furthermore, we tried to validate our results in a cohort of DRE patients who underwent CM-DBS or CM-RNS (responsive neurostimulation). We hypothesized that the sweet-spot would share similar structural connectivity with responder patients.
Methods: By using the software FMRIB Software Library (FSL), probabilistic tractography was performed on 100 subjects from the Human Connectome Project to calculate the probability of connectivity of the whole CM, the sweet-spot and the cold-spot to 45 cortical and subcortical areas. Results among the three seeds were compared with multivariate analysis of variance (MANOVA). Similarly, the structural connectivity of volumes of tissue activated (VTAs) from eight DRE patients was investigated. Patients were divided into responders and non-responders based on the degree of reduction in seizure frequency, and the mean probabilities of connectivity were similarly compared between the two groups.
Results: The sweet-spot demonstrated a significantly higher probability of connectivity ($p < 0.001$) with the precentral gyrus, superior frontal gyrus, and the cerebellum than the whole CM and the cold-spot. Responder patients displayed a higher probability of connectivity with both ipsilateral ($p = 0.011$) and contralateral cerebellum ($p = 0.04$) than the non-responders.
Conclusion: Cerebellar connections seem to contribute to the beneficial effects of CM-neuromodulation in patients with drug-resistant generalized epilepsy.

Keywords: centromedian nucleus, cerebellum, deep brain stimulation, epilepsy, responsive neurostimulation

Correspondence to:
Luigi G. Remore
Surgical Neuromodulation and Brain Mapping Laboratory, ULCA

Department of Neurosurgery, 300 Stein Plaza, Los Angeles, CA 90095, USA

University of Milan 'La Statale', Milan, Italy

Department of Neurosurgery, Fondazione IRCCS Ca'Granda Ospedale Maggiore Policlinico, Milan, Italy
luigigianmaria.remore@ gmail.com

Ziad Rifi
Department of Neurosurgery, University of California Los Angeles, Los Angeles, CA, USA

Hiroki Nariai
Division of Pediatric Neurology, Department of Pediatrics, University of California Los Angeles, Los Angeles, CA, USA

David Geffen School of Medicine, University of California Los Angeles, Los Angeles, CA, USA

Dawn S. Eliashiv
David Geffen School of Medicine, University of California Los Angeles, Los Angeles, CA, USA

Department of Neurology, University of California Los Angeles, Los Angeles, CA, USA

Aria Fallah
Department of Neurosurgery, University of California Los Angeles, Los Angeles, CA, USA

Division of Pediatric Neurology, Department of Pediatrics, University of California Los Angeles, Los Angeles, CA, USA

David Geffen School of Medicine, University of California Los Angeles, Los Angeles, CA, USA

Benjamin D. Edmonds
Joyce H. Matsumoto
Division of Pediatric
Neurology, Department
of Pediatrics, University
of California Los Angeles,
Los Angeles, CA, USA

Noriko Salamon
David Geffen School of
Medicine, University of
California Los Angeles,
Los Angeles, CA, USA

Department of Radiology,
University of California
Los Angeles, Los
Angeles, CA, USA

Meskerem Tolossa
Wexin Wei
Department of
Neurosurgery, University
of California Los Angeles,
Los Angeles, CA, USA

Marco Locatelli
University of Milan 'La
Statale', Milan, Italy

Department of
Neurosurgery,
Fondazione IRCCS
Ca'Granda Ospedale
Maggiore Policlinico,
Milan, Italy

Department of
Pathophysiology and
Transplantation,
University of Milan, Milan,
Italy

'Aldo Ravelli'
Research Center for
Neurotechnology and
Experimental Brain
Therapeutics, University
of Milan, Milan, Italy

Evangelia C. Tsolaki
Department of
Neurosurgery, University
of California Los Angeles,
Los Angeles, CA, USA

Ausaf A. Bari
Department of
Neurosurgery, University
of California Los Angeles,
Los Angeles, CA, USA

Geffen School of Medicine
David California Los
Angeles University of
Angeles Los CA, USA

* These authors
contributed equally

Introduction

Epilepsy is a common chronic neurological disorder with an estimated pooled incidence rate of 61.4 per 100,000 people per year.[1] Antiepileptic drugs are the first line of therapy, but up to 30% of patients fail to respond to multiple or combined pharmacological therapies and are diagnosed with drug-resistant epilepsy (DRE).[2] Moreover, approximately half of DRE patients are not suitable candidates for resective surgery, which is known to have a high seizure freedom rate.[3] For this cohort of patients, neuromodulation targeting the thalamus has been investigated as a promising surgical treatment.[4] In recent years, deep brain stimulation (DBS) of the anterior nucleus of the thalamus was approved in Europe and the United States as adjunctive therapy for the treatment of patients suffering from focal seizures with or without secondary generalization and refractory to three or more antiepileptic medications.[5,6] Conversely, all the neuromodulatory techniques for the treatment of generalized epilepsy remain off-label.[7–9] In this context, DBS targeting the centromedian nucleus (CM) of the thalamus seems to be particularly promising in patients suffering from generalized DRE epilepsy. The first case series of CM-DBS for the treatment of generalized DRE dates back to 1987 by Velasco *et al.*,[10] who reported a significant reduction of clinical seizures after 3 months of cyclic stimulation in five patients suffering from generalized DRE. Following this first report, a recent meta-analysis[11] demonstrated a mean seizure reduction rate of 73.4% after a mean follow-up of 28.7 months. Similarly, responsive neurostimulation (RNS) of CM has been proposed as an alternative approach to control generalized seizures by some USA centers and showed encouraging results.[12–14]

The CM is a small thalamic region measuring less than 10 mm in every dimension with an approximately 310 mm^3 volume.[15] It belongs to the caudal intralaminar group of thalamic nuclei and is situated within the medial thalamus bordered superiorly by the mediodorsal nucleus, medially by the parafascicular nucleus (Pf), and posteriorly by the pulvinar.[16] The first tracing studies of CM were performed on rats, in which this nucleus is indistinguishable from Pf.[17] Based on this methodology, CM was described as the principal target of projections from the mesencephalic reticular formation and the main source of extracortical afferents to the basal ganglia. Therefore, murine CM was considered a pivotal regulator of motor task performance in the cortical–basal ganglia–thalamo–cortical loop. Similar anatomical studies in primates[18] showed that CM was well distinguishable from Pf and demonstrated predominant connections to frontal, prefrontal, and parietal cortices. On the other hand, the primate Pf displayed a more limbic pattern of cortical and subcortical connections. Given its widespread cortical and subcortical connections and the electrophysiologic evidence of diffuse EEG desynchronization produced by active CM stimulation,[19] Velasco's group proposed that neuromodulation of the centromedian nucleus would be useful for the management of different types of generalized epileptic syndromes.

Recently, Warren *et al.*[20] performed a volume of tissue activated (VTA)-based probabilistic map analysis on a cohort of 20 Lennox–Gastaut syndrome (LGS) patients from the Electrical Stimulation of Thalamus for Epilepsy of Lennox–Gastaut phenotype (ESTEL) tiral.[21] In this first monocentric randomized-control study, the authors evaluated the clinical efficacy of CM-DBS in patients with LGS, which is a specific subtype of generalized epilepsy. They also generated a sweet-spot and a cold-spot, defined as thalamic subregions where the stimulation yielded above-mean and below-mean seizure frequency reduction, respectively. Interestingly, the sweet-spot covered the anterolateral portion of CM, but it also extended to the posterior subdivision of the ventrolateral nucleus based on the Krauth *et al.*/Morel histological atlas.[22] In the current study, we conducted a probabilistic tractography analysis to elucidate the structural connectivity of CM. Then, we compared these connections with those of the recently described sweet- and cold-spots to find possible differences in connectivity that would explain the anti-seizure effect from CM-neuromodulation. Finally, we tried to validate our results in a cohort of eight patients suffering from chronic generalized DRE, who underwent CM-DBS or CM-RNS. Our hypothesis is that a similar connectivity pattern may be shared by the sweet-spot and the responder patients.

Material and methods

Study subjects

We used 'minimally pre-processed' 100 unrelated subjects (58 females, 42 males; mean age = 27) from the Human Connectome Project (HCP) database[23] (http://humanconnectome.org), whose

acquisition and pre-processing are described elsewhere.[24] The results from HCP subjects were then validated in a cohort of eight patients suffering from chronic generalized DRE who underwent neuromodulation surgery. Our cohort was composed of two different populations: three adult patients (≥18 years of age) diagnosed with DRE according to the International League Against Epilepsy (ILAE) guidelines[25] by the attending neurologists at UCLA Ronald Regan Medical Center and five pediatric patients (<18 years of age), whose diagnosis was made by attending pediatric neurologists at UCLA Mattel Children's Hospital. Of all patients, six underwent CM-RNS and 2 CM-DBS. The choice between DBS and RNS was guided by the expertise and the preference of the attending neurologist caring for the patient. Clinical and imaging data were retrospectively collected from the clinical database of our institution.

### Patients' MRI data acquisition and pre-processing

Before surgery, each patient underwent 3 T magnetic resonance imaging (MRI) on a Siemens Prisma scanner, including T1-weighted anatomical images using the MP-RAGE sequence (TE = 2.98 ms, TR = 2.5 s, matrix = 256 × 256, isotropic 1 mm voxels, and flip angle = 15°) and single-shot spin-echo echo planar imaging for diffusion tensor imaging (TE = 91 ms, TR = 7.6 s, matrix = 128 × 128, voxel size = 1.7 mm × 1.7 mm or 2 mm × 2 mm, slice thickness = 2, b-value = 1000, and 64 directions). MRI scans of pediatric patients were acquired under general anesthesia.

For each patient, T1 images were skull stripped (BET)[26] and nonlinearly co-registered to the MNI152 space by using FNIRT tool in FMRIB Software Library (FSL) (ver. 5.0; http://fsl.fmrib.ox.ac.uk/fsl).[27] Eddy current correction was then used to apply affine registrations to each volume in the diffusion dataset and register it with the initial reference B0 volume. Before performing tractography, all diffusion data were processed using Bayesian Estimation of Diffusion Parameters Obtained Using Sampling Techniques (BEDPOSTX),[28,29] which runs Markov Chain Monte Carlo sampling to build up distributions of diffusion parameters at each voxel. Then, a multi-fiber diffusion model was fitted on HCP data by using the FMRIB's Diffusion (FDT) toolbox in FSL.[29] This model uses Bayesian techniques to estimate a probability distribution function (PDF) on the principal fiber direction at each voxel, accounting for the possibility of crossing fibers within each voxel. Three fibers were modeled per voxel, a multiplicative factor of 1 for the prior on the additional modeled fibers and 1000 iterations before sampling.[28] Finally, DTI data were linearly co-registered to the structural T1 images by using FLIRT tool and nonlinearly co-registered to the standard MNI space as described above.

Surgical technique

All patients or their legal representatives gave written informed consent for the surgical procedure. For adult patients, the CM was initially targeted indirectly based on stereotactic coordinates as reported in the literature[30,31] (x = 8–10 mm lateral to the midcommissural point, y = 1 mm anterior to the posterior commissure, z = 0–1 mm superior to the intercommissural plane). The stereotactic target was then adjusted according to the patient's anatomy on the T1-weighted sequence. For pediatric patients, the CM was manually segmented by an attending neuroradiologist (NS) based on the T1-weighted image. For all patients, the lead trajectory was chosen on the gadolinium-enhanced T1-weighted sequence. The remaining steps of the surgical procedure were similar in the two patient populations, although surgeries were performed by two different attending neurosurgeons (AAB for the adult patients and AF for the pediatric patients). Under general anesthesia, a Leksell stereotactic frame (Elekta, Stockholm, Sweden) was applied to the patient's head and a thin-cut stereotactic CT was obtained. In a dedicated workstation (Elements, BrainLab, Kapellenstrat, Germany) the CT scan was co-registered with MRI sequences containing the stereotactic plan. SenSight directional leads (Sensight Model B33005, Medtronic Inc., Minneapolis, MN, USA) and four-contacts depth leads (DL-330-3.5, NeuroPace, Mountain View, CA, USA) were bilaterally implanted for CM-DBS and CM-RNS patients, respectively. For CM-RNS patients, the RNS Neurostimulator (model RNS-300M, NeuroPace, Mountain View, CA, USA) was implanted into the skull during the same surgical procedure. On the other hand, CM-DBS patients were discharged the following day and returned as outpatients after 1 week to implant the extension leads and a Percept PC IPG (Medtronic Inc., Minneapolis, MN, USA).
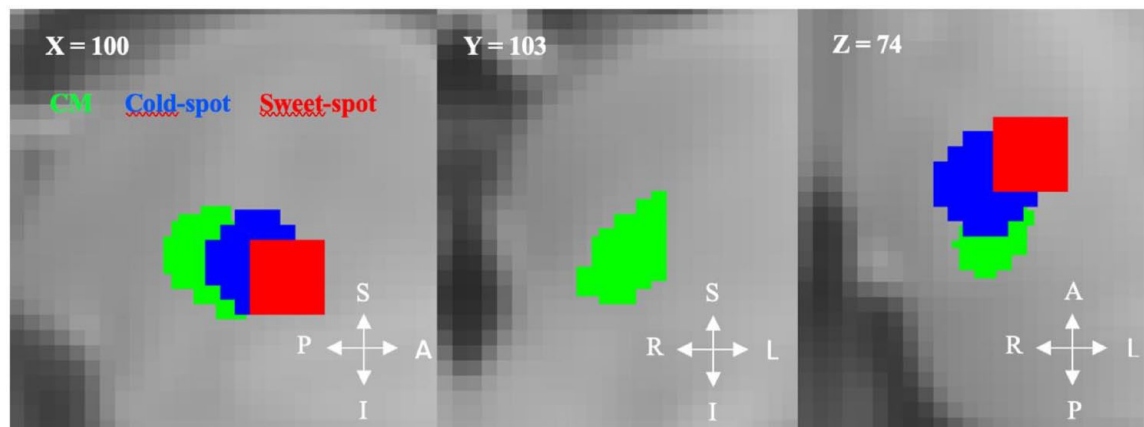
Figure 1. Seeds employed for tractography analysis in HCP subjects.
From left to right, the three seeds are displayed on the sagittal, coronal, and axial planes. The centromedian nucleus (CM) is depicted in green, the cold-spot in blue, and the sweet-spot in red. Note the more inferior, anterior, and lateral locations of the sweet-spot relative to CM.
A, anterior; HCP, human connectome project; I: inferior; L, left; P, posterior; R, right; S, superior.

Afterward, stimulation parameters were programed during the following neurologic outpatient clinic.

VTAs reconstruction

For each patient, left VTAs were computed using the stimulation parameters (active contacts and amplitude in mA) as recorded at the last follow-up visit. VTAs were estimated using the finite element method (FEM)-based FieldTrip SimBio pipeline in Lead-DBS (ver. 2.6).[32] As reported by previous studies,[33,34] VTAs were modeled assuming a homogenous tissue conductivity of 0.1 S/m and thresholded to binary three-dimensional volumes by applying an electric field cutoff of 0.2 V/mm to approximate the gold standard of axon cable models.[35]

Tractography seeds and targets

For HCP subjects, three seeds were chosen for the tractography analysis: a left CM mask from the THOMAS atlas[36] and two 3-mm-radius spherical ROI generated in MNI125 space with the Gaussian Kernel function based on the MNI coordinates of the cold- and sweet-spots as reported by Warren *et al.*[20] (Figure 1). We chose to analyze only the connections of the left CM to be consistent with the findings from the study by Warren *et al.*[20] In fact, these authors mirrored all VTAs from their patients to the left and conducted the whole analysis for the left hemisphere. Therefore, Warren *et al.* reported only the left coordinates for both the sweet- and cold-spot in the original paper.[20] Moreover, we did not expect significant differences in the connectivity between the left and right CM because the beneficial effect of unilateral CM stimulation has been known since the first reports by Velasco *et al.*'s group[31] and even other authors employed unilateral CM-DBS with good seizure control.[37] All three masks were co-registered to the subject diffusion space. When analyzing the connectivity of the eight DRE patients, previously generated VTAs were used as seeds after co-registration with patients' diffusion space. For both HCP subjects and DRE patients, FreeSurfer (v6.0; http://surfer.nmr.mgh.harvard.edu)[38] was used for cortical surface reconstruction and volumetric segmentation to automatically generate target areas for the tractography analysis.[34–36] Forty-five target areas were chosen and divided into five groups: infratentorial, basal ganglia, sensorimotor, associative, and limbic. The complete list of target areas for each group is presented in Supplemental Table S1.

Probabilistic tractography

For HCP subjects, probabilistic tractography was performed to delineate the structural connectivity between the CM mask, and the cold- and sweet-spot with the target areas. Using the PDFs previously calculated and the PROBTRACKX
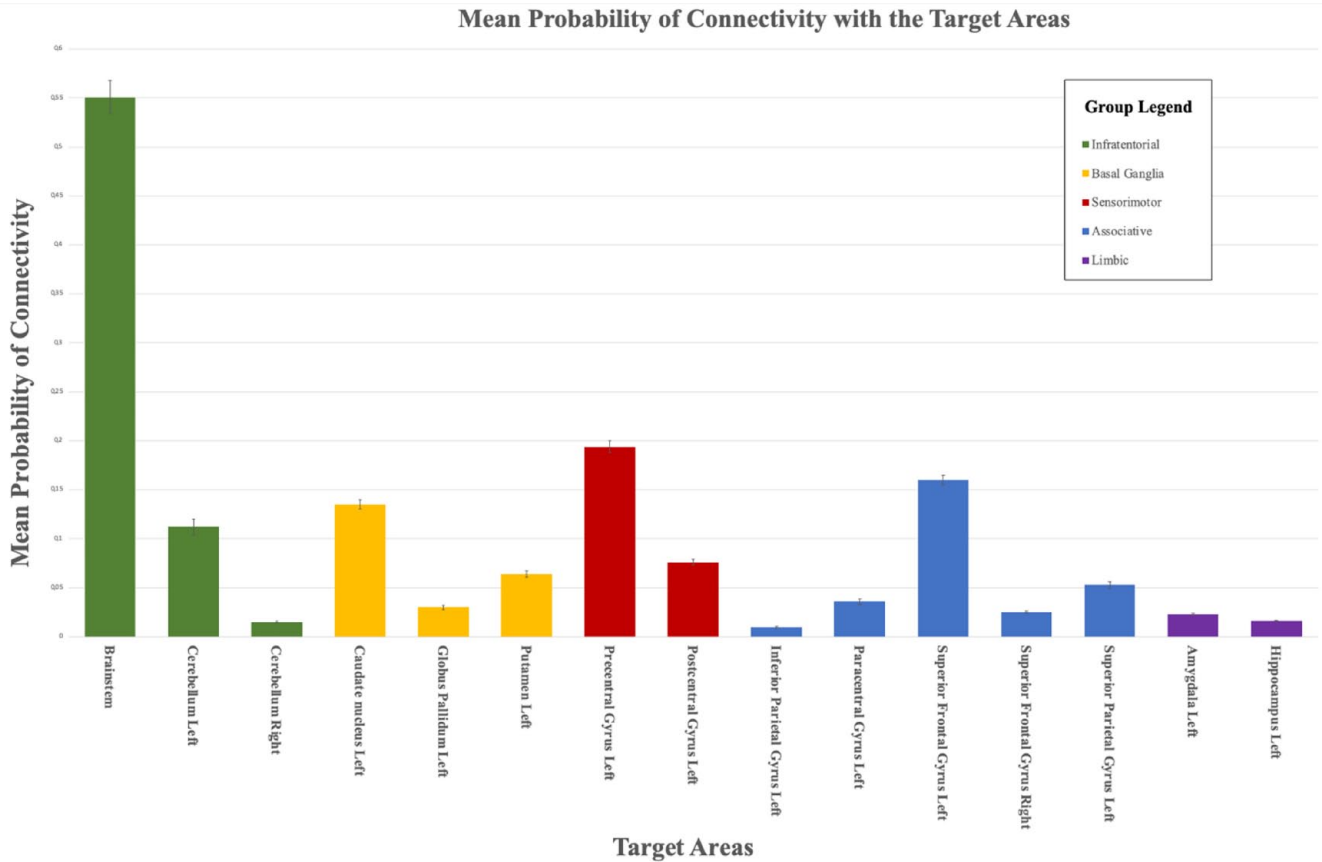
Figure 2. Mean probability of connectivity of left CM seed with the selected target areas.
The bar graph shows the 15 reliable connections identified for CM proper. As explained in the main text, the probability of connectivity describes the probability that a particular voxel lies on an existing tract. Only connections with a probability of connectivity >0.01 were selected for the following analysis. As exemplified by the color-coded connections, CM demonstrated a higher probability of connectivity with the brainstem for the infratentorial group, the caudate for the basal ganglia group, the precentral gyrus for the sensorimotor group, the superior frontal gyrus for the associative group, and the amygdala for the limbic group.

function,[24,25] we determined the probability of connectivity between each seed and the target areas. From each voxel in the three seed masks, we used the following parameters: 5000 streamlines generated, a 0.2 curvature threshold, and a loop check termination. All the target masks were used as waypoint masks to discard tracts not passing through the target, termination masks to terminate the pathways as soon as they reach the target, and classification masks to quantify connectivity values between the seed and target mask.[29] To measure the strength of connectivity between regions, we used the probability of connectivity, which is defined as the probability that a particular voxel lies on an existing tract. For each seed, the probability of connectivity to each target area was calculated by dividing the number of streamlines connecting the seed to the target area by the total number of streamlines sent out (5000 streamlines per seed voxel),[39,40] according to the following formula:

$$\text{Probability of Connectivity} = \left(\frac{\text{Number of streamlines that connected to target}}{\text{Number of Seed Voxels that connected to target} \times 5000} \right)$$

To compensate for the distance-dependent effect, all the calculated probabilities of connectivity were corrected by the average distance of the seed to the corresponding target area.[41,42] Furthermore, connections with null or sub-threshold ($p > 0.01$) probability of connectivity were regarded as false-positive results[43] and not included in the following analysis. Similarly, we calculated the corrected probability of connectivity of patients' left VTA with the target areas resulted statistically significantly different in the previous analysis. Then, the patients were divided into responders and non-responders using as response criterion $a > 50\%$ seizure frequency reduction as evaluated by the attending neurologists at the last follow-up visit. Finally, the VTAs probability of connectivity with the target areas was compared between responders and non-responders.

Statistical analysis

Descriptive statistics, frequencies, and percentages were used to report demographic characteristics. A Shapiro–Wilk normality test was used to assess normality across selected variables along with a close inspection of the data plotted on histograms and Q–Q graphs. Continuous variables were reported as mean plus standard deviation. Categorical variables were reported as absolute numbers and percentages. In HCP subjects, MANOVA was employed to perform multivariate comparisons for the mean probability of connectivity among the three seeds (CM, sweet-spot, cold-spot). In this context, the Pillai–Bartlett trace (V) multivariate test was used as a test for overall statistical significance among all variables and ANOVA univariate F-statistic as a follow-up test in case of multivariate significance. Finally, two *post hoc* tests were used to uncover specific differences in the statistically significant connections among the three seeds: Bonferroni if Levene's test of equality of error variances was not violated and Games–Howell in the case of Levene's test violation. Continuous variables in the patients' cohort were non-normally distributed, and the Quade's non-parametric ANCOVA was used to compare means between responders and non-responders while correcting for patients' age. For all traditional hypotheses, p values <0.05 were considered statistically significant. Statistical analysis was performed using SPSS (version 28.0, IBM, Armonk, NY, USA).

Results

Based on the probability of connectivity to target areas, 15 reliable connections were identified for CM (Supplemental Table S2; Figure 2). Overall, the CM had higher connectivity with the brainstem, pre- and postcentral gyri, superior frontal gyrus, caudate nucleus, and cerebellum. Interestingly, the CM displayed bilateral connections with the superior frontal gyrus and the cerebellum, although ipsilateral connections were predictably higher. When considering each target group separately, the CM had a higher probability of connectivity with the brainstem for the infratentorial group, the caudate for the basal ganglia group, the amygdala for the limbic group, the precentral gyrus for the sensorimotor group, and the superior frontal gyrus for the associative group.

Comparison among the three seeds in HCP subjects

The multivariate test was statistically significant [$V = 0.791$, $F(32,566) = 11.565$, $p < 0.001$], and the follow-up univariate analysis confirmed significant differences among the three seeds for the connections with the following structures (Table 1): the brainstem and the contralateral cerebellum; the ipsilateral globus pallidus and the putamen; the ipsilateral precentral and postcentral gyri; the ipsilateral and contralateral superior frontal gyri, the ipsilateral superior parietal gyrus, and the inferior parietal gyri; the amygdala.

The *post hoc* test (Supplemental Table S3; Figure 3) revealed that the CM proper had a statistically significantly higher probability of connectivity with the brainstem than the sweet-spot ($p < 0.001$) and the cold-spot ($p = 0.004$) but a lower one with the ipsilateral superior frontal gyrus than the other two seeds ($p < 0.001$). When directly comparing the sweet-spot with the other two seeds, a higher probability of connectivity was demonstrated with the contralateral cerebellum ($p < 0.001$ for both comparisons), the ipsilateral precentral gyrus ($p < 0.001$ for both comparisons), and the contralateral superior frontal gyrus (comparison with CM: $p = 0.01$; comparison with the cold-spot: $p < 0.001$), but lower connectivity was found with the globus pallidum (comparison with CM: $p = 0.005$; comparison with the cold-spot: $p < 0.001$) and the postcentral gyrus ($p < 0.001$ for both comparisons). Finally, the

Table 1. Mean probability of connectivity of the three seeds with the selected target areas for HCP subjects.

Target areas	CM	Cold-spot	Sweet-spot	F[a]	*p* Value[a]
Infratentorial group					
Brainstem	0.552 ± 0.165	0.431 ± 0.159	0.483 ± 0.133	15.72	<0.001*
Cerebellum left	0.112 ± 0.008	0.093 ± 0.006	0.115 ± 0.006	2.82	0.061
Cerebellum right	0.015 ± 0.01	0.012 ± 0.009	0.023 ± 0.013	21.9	<0.001*
Basal Ganglia group					
Caudate nucleus left	0.135 ± 0.005	0.142 ± 0.005	0.137 ± 0.006	0.43	0.65
Globus pallidum left	0.04 ± 0.001	0.04 ± 0.002	0.03 ± 0.001	8.34	<0.001*
Putamen left	0.064 ± 0.003	0.076 ± 0.037	0.065 ± 0.039	3.19	0.043*
Sensorimotor group					
Postcentral gyrus left	0.076 ± 0.003	0.069 ± 0.004	0.047 ± 0.003	16.11	<0.001*
Precentral gyrus left	0.194 ± 0.006	0.197 ± 0.058	0.281 ± 0.062	63.23	<0.001*
Associative group					
Inferior parietal gyrus left	0.01 ± 0.001	0.007 ± 0.06	0.007 ± 0.05	3.97	0.022*
Paracentral gyrus left	0.036 ± 0.003	0.03 ± 0.003	0.0365 ± 0.003	1.59	0.204
Superior frontal gyrus Left	0.16 ± 0.005	0.2 ± 0.005	0.21 ± 0.006	15.42	<0.001*
Superior frontal gyrus right	0.025 ± 0.001	0.023 ± 0.001	0.031 ± 0.001	8.92	<0.001*
Superior parietal gyrus left	0.053 ± 0.003	0.022 ± 0.002	0.029 ± 0.001	23.82	<0.001*
Limbic group					
Amygdala left	0.023 ± 0.001	0.026 ± 0.0016	0.02 ± 0.0014	3.38	0.035*
Hippocampus left	0.016 ± 0.007	0.017 ± 0.0009	0.014 ± 0.0007	2.89	0.07

*$p < 0.005$ was considered statistically significant.
[a]F-statistics and *p*-value reported from comparison among probabilities of connectivity of the three seeds by using ANOVA.

cold-spot had a higher probability of connectivity with the putamen than the two other seeds (comparison with CM: $p < 0.001$; comparison with the sweet-spot: $p = 0.005$) and with the amygdala ($p = 0.027$) than the sweet-spot, but cold-spot connectivity with the brainstem was significantly lower ($p = 0.036$) than the sweet-spot.

Patient cohort
The patient cohort was composed of eight subjects diagnosed with DRE. (Table 2). Six patients (75%) underwent CM-RNS and two (25%) received CM-DBS. Most were female (62.5%), whereas the mean age at epilepsy onset and at surgery was 4.59 ± 4.322 years and 19.8 ± 17.09 years, respectively. Five patients had vagus nerve stimulator (VNS) implanted before undergoing CM-neuromodulation, but none had previous resective surgery since they were not deemed suitable candidates. After a mean post-implantation follow-up of 9.5 ± 3.84 months, the mean percentage reduction of seizure frequency was 60.5 ± 34.8%. However, four patients were considered responders as they achieved >50% seizure frequency reduction at the last follow-up
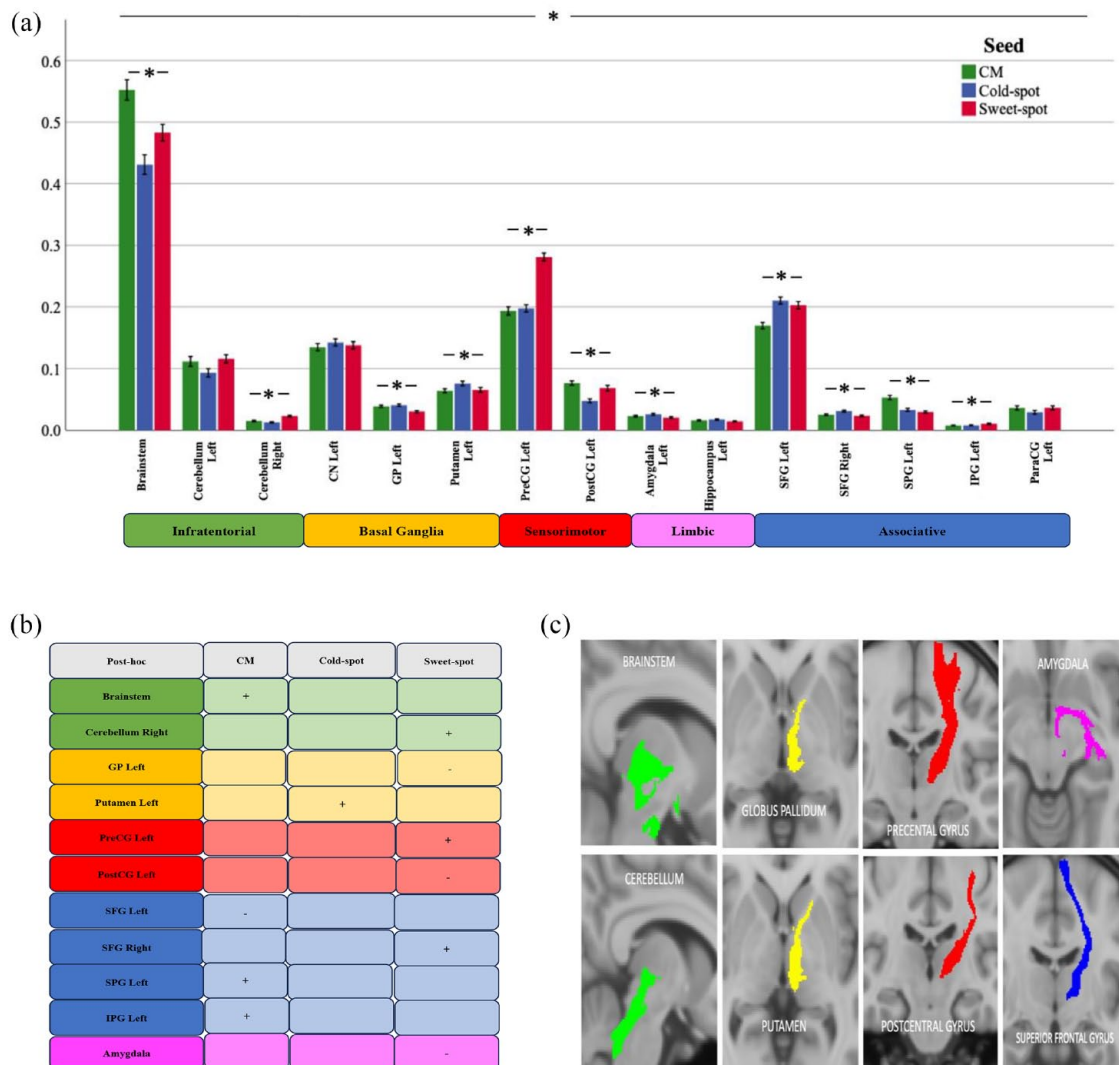
Figure 3. Main analysis for the HCP subjects. (a) The bar chart shows the statistically significant differences found among the selected connections for the HCP subject both at a multivariate and univariate level. On the *x* axis, the connections are classified according to the defining group. (b) The table exemplifies the results of the *post hoc* test for the three seeds. The signs '+' and '−' indicate the statistically significantly higher or lower probabilities of connectivity, respectively. (c) Major tracts for each group of connections are displayed in MNI space 152. *Statistically significant differences (*p* < 0.05).
CN, caudate nucleus; GP, globus pallidum; HCP, human connectome project; IPG, inferior parietal gyrus; ParaCG, paracentral gyrus; PreCG, precentral gyrus; PostCG, postcentral gyrus; SFG, superior frontal gyrus; SPG, superior parietal gyrus.

visit with a mean percentage of seizure frequency reduction of $88.5 \pm 7.8\%$ against $32.5 \pm 11\%$ in non-responders ($p = 0.006$). Three out of four responders (75%) were LGS patients, whereas all the non-responders were non-LGS.

When comparing the connectivity of VTAs between responders and non-responders with the previously identified target areas (Table 3),

responder patients demonstrated a significantly higher probability of connectivity with the ipsilateral ($p = 0.011$) and contralateral cerebellum ($p = 0.04$). Furthermore, higher connectivity was found with the precentral gyrus, the ipsilateral and contralateral superior frontal gyri in responder patients and with the amygdala, the globus pallidum, the putamen, the postcentral gyrus, and the superior parietal gyrus in non-responder patients.

Table 2. Clinical characteristics of the patients with chronic generalized epilepsy in the present study.

Patient	Sex[a]	Age at onset[b]	Age at implantation[c]	Epilepsy/Seizure type	Epilepsy etiology	Stimulation type	Stimulation settings
1	F	8	60	Tonic-clonic	Undefined[d]	RNS	Bipolar
2	M	1.25	3.6	LGS	Genetic	RNS	Bipolar
3	F	2	13	Myoclonic	Undefined[d]	RNS	Bipolar
4	M	0.5	9	LGS	Undefined[d]	RNS	Bipolar
5	M	1.5	16.5	LGS	Undefined[d]	RNS	Bipolar
6	F	1.5	6	Tonic-clonic	Genetic	RNS	Bipolar
7	F	10	30	JAE	Genetic	DBS	Monopolar
8	F	12	20	Tonic-clonic	Undefined[d]	DBS	Monopolar

[a]Patient's sex (*M*=male, *F*=female); [b]patient's age at seizures onset expressed in years; [c]patient's age at implantation expressed in years; [d]epilepsy etiology was deemed to be 'undefined' after a thorough clinical workout, including careful anamnesis and physical examination, different neuroimaging studies (MRI and PET), video-EEG and stereo-EEG in selected cases.
JAE, Juvenile Absence Epilepsy; LGS, Lennox–Gastaut syndrome; RNS, responsive neurostimulation.

Table 3. Mean probability of connectivity for patient's left VTA with the selected target areas.

Target area	Responders[a]	Non-responders	*p* Value
Amygdala left	0.001 ± 0.001	0.006 ± 0.005	0.726
Brainstem	0.665 ± 0.084	0.656 ± 0.142	0.89
Cerebellum left	0.252 ± 0.111	0.058 ± 0.017	0.011*
Cerebellum right	0.011 ± 0.006	0.001 ± 0.002	0.04*
Globus pallidum left	0.013 ± 0.01	0.066 ± 0.04	0.488
Precentral gyrus left	0.224 ± 0.1	0.198 ± 0.088	0.348
Postcentral gyrus left	0.037 ± 0.02	0.176 ± 0.144	0.544
Putamen left	0.021 ± 0.012	0.107 ± 0.1	0.455
Superior frontal gyrus left	0.165 ± 0.117	0.095 ± 0.077	0.188
Superior frontal gyrus right	0.011 ± 0.004	0.003 ± 0.008	0.101
Superior parietal gyrus left	0.005 ± 0.004	0.02 ± 0.01	0.135

[a]Response to stimulation is defined as >50% seizure frequency reduction as evaluated by the attending neurologists at the last follow-up visit.
*$p < 0.005$ was considered statistically significant.

Finally, no differences resulted in the connections with the brainstem ($p = 0.89$) and no connections at all ($p = 0$) with the inferior parietal gyrus in all the patients.

Discussion

Our probabilistic tractography study demonstrated that the CM had the strongest structural connectivity with the brainstem, basal ganglia, cerebellum, primary motor and sensory cortices, and the prefrontal cortex, confirming non-human tract tracing studies.[16,18] This widespread connectivity pattern supports the involvement of the primate CM in brain functions other than motor regulation (such as attention, arousal,[44] and nociception[45]). In fact, CM-neuromodulation has been investigated for the treatment of different neuropsychiatric pathologies such as Tourette's syndrome,[46] neuropathic pain,[47] coma, and other vegetative states.[48] On the other hand, weaker structural connections of CM with limbic structures resulted, except for the amygdala and the hippocampus. When investigating possible differences in structural connectivity among the CM proper and the cold- and sweet-spots as described by Warren *et al.*,[20] we demonstrated that the sweet-spot had a significantly higher probability of connectivity with the ipsilateral precentral gyrus (primary motor cortex), the brainstem, and the contralateral superior frontal gyrus and cerebellum, but lower connectivity with the postcentral gyrus (primary sensory cortex) and the superior and inferior parietal gyri.

We then confirmed these findings in a cohort of 8 DRE patients who underwent CM-neuromodulation, since VTAs from responders had a pattern of connections similar to the sweet-spot. Our results are in accordance with the analysis by Warren *et al.*,[20,49] who showed that probabilistic CM maps associated with increased seizure reduction were more strongly connected with the cerebellum and frontal areas than with parietal cortices. Interestingly, histological tracing studies indicated that most fibers connecting the CM with frontal cortices and the cerebellum were located in its inferolateral part, which is histologically known as the 'parvocellular' component (pvCM) and has been indicated as the targeting site associated with the best clinical outcome by previous studies.[31,50] Therefore, it is not surprising that the sweet-spot described by Warren *et al.*[20] was located on the border between pvCM

and the posterior subdivision of the ventral lateral nucleus, which also receives afferents from the cerebellum and projects to the motor and premotor cortices.[51] In fact, the current literature agrees in assigning the frontal cortex an important pathophysiological role in generalized epilepsy.[52,53] In particular, it has been shown that the inhibition threshold of neurons within the motor cortex is higher in patients with generalized epilepsy than in both healthy subjects and patients with focal epilepsy.[54] Moreover, non-invasive motor cortex recording in epileptic patients who underwent ANT-DBS demonstrated increased intracortical inhibition[55] and encouraging clinical results were reported in closed-loop stimulation targeting the motor cortex in some cases of medically and surgical refractive epilepsy.[56,57] On the other hand, structural and functional alterations involving the superior frontal gyrus have been related to ictal activity in various epileptic syndromes.[58,59] More recently, an anatomic parcellation of the superior frontal gyrus has been proposed, encompassing three subregions[43,60]: an anteromedial component connected to the anterior cingulate cortex and other limbic areas; a dorsolateral component connected with the middle and inferior frontal gyri; and a posterior component connected to the motor cortex and the basal ganglia. Based on this classification, the superior frontal gyrus can access many cortical and subcortical sites and might be a relevant hub for seizure initiation or spreading in generalized epilepsy.

Among CM connections, the cerebellar ones seem to have a particularly promising role in seizure control. In fact, we found stronger cerebellar connections with the sweet-spot and this finding was confirmed in responder patients, who displayed a statistically significant higher probability of connectivity with the cerebellum bilaterally than non-responder patients. The cerebellum has widespread connections[61,62] and is now known to take part in brain functions other than sensorimotor regulation, such as language, cognition, and emotion.[63] The role of the cerebellum in epilepsy had initially been suggested by anecdotal reports of cerebellar lesions causing seizures reversible with surgery[64] and post-mortem anatomical abnormalities found in the cerebellum of epilepsy patients with varying etiologies.[65,66] More recently, neuroimaging studies have reported increased cerebellar activity during and after seizures[67] and identified altered cerebellar functional

connectivity as a predictor of drug resistance in epileptic patients.[68] Stemming from these findings, stimulation of the cerebellar cortex was one of the first neuromodulatory approaches used to treat DRE,[69] but it yielded disappointing results.[70–72] A possible explanation is that the complex foliation of the cerebellar cortex and its compartmentalization into functional zones (i.e. the zebrin bands) may cause a nonspecific spread of electrical stimulation.[51] As a result, the attention of researchers shifted toward the deep cerebellar nuclei, which receive converging afferents from cortical Purkinje cells and are directly connected with many brainstem and thalamic nuclei.[73] In fact, recent murine models of epilepsy showed that direct optogenetic activation of deep cerebellar nuclei can effectively stop both primary generalized[74] and hippocampal-onset seizures.[75] The tract connecting the CM with the cerebellar white matter in our analysis runs through the superior cerebellar peduncle (i.e. brachium conjunctivum), which is the output of the cerebellar dentate nucleus. Interestingly, functional connectivity between this nucleus and the primary motor cortex was altered in a recent study on patients with generalized epilepsy with unknown etiology.[76] Taken together, this evidence strengthens the idea that activation of cerebellar nuclei may stop seizure activity, perhaps by desynchronizing a wide array of subcortical and cortical structures via their widespread polysynaptic connections.[77] These conclusions assume particular importance if considering that our patient cohort was composed of both adult and pediatric subjects with different epileptic syndromes not limited to LGS. Consequently, CM connections with the cerebellum might positively impact seizure control irrespective of epilepsy etiology.

On the other hand, the role of the connections with the brainstem and the basal ganglia was not completely elucidated by our analysis. In fact, the CM displayed the highest probability of connectivity with the brainstem, but its projections seem to involve mainly the mesencephalon and the pons. The relevance of the brainstem in seizure spreading has been known since the first electrophysiologic studies in animals,[78] and its importance in the pathophysiology of epilepsy disorders other than LGS (such as generalized absence seizures[79]) is acknowledged. Although many brainstem nuclei have been involved in epilepsy pathophysiology (such as the subthalamic nucleus,[80] the superior colliculus,[81] and the

cholinergic reticular nuclei[82]), the exact role of each nucleus in seizure generation or spreading is still unclear. Since the sweet-spot had stronger connections with the brainstem than the cold-spot, our work seemed to agree with previous findings[20,49,83] in correlating CM connectivity to the brainstem with positive clinical outcomes. However, the probability of connectivity with the brainstem was almost identical between responder and non-responder patients. On the contrary, the results from HCP subjects would suggest a negative role for the connections with the basal ganglia, since the cold-spot in our analysis demonstrated higher connectivity with the globus pallidus and the putamen than the sweet-spot. By performing a VTA-based analysis similar to Warren *et al.*[20,49] on a cohort formed by patients with different generalized epileptic syndromes, Torrez-Diaz *et al.*[83] demonstrated a negative correlation between seizure reduction after CM-DBS and structural connectivity with the basal ganglia, whereas Warren *et al.*[20,49] found the opposite. These findings strengthened the emerging idea that different generalized epileptic syndromes would benefit from the stimulation of different CM sub-components, since a diverse connectivity pattern may underlie each seizure pathophysiology.[84] In fact, the same authors from the ESTEL trial formulated a cortically driven theory for LGS pathophysiology,[59,85] centered on early generated paroxysmal fast activity in prefrontal cortices and their subsequent propagation via the extrapyramidal corticoreticular pathway to the brainstem and basal ganglia. Therefore, it is reasonable that LGS patients would benefit the most from stimulation of pvCM, which is mainly connected with the frontal and prefrontal areas.[86] Even in our cohort, all LGS patients were responders. However, the differences in basal ganglia connectivity between responders and non-responders in our patients' cohort were not statistically significant, and the role of basal ganglia connectivity remains unclear.

Limitations

The main limitation of probabilistic tractography analysis is the rate of false-positive tracts, which is common to the algorithms so far employed and particularly relevant when a whole-brain approach is selected.[87] Consequently, we chose a targeted-based approach by using an MRI-validated CM mask as seed. Nonetheless, the targeted tractography strategy is inherently biased by a priori

anatomical knowledge of white matter tracts.[88] To overcome this limitation, we selected as target areas a wide array of anatomical structures spanning beyond the current evidence in the literature. Moreover, the DRE patient cohort we analyzed to validate our connectivity results was composed of a relatively small number of subjects, who were also heterogenous based on age and epilepsy etiology, programming settings, and CM targeting strategies. Although cerebellar connections were stronger in both the sweet-spot and responder patients, further studies with a larger cohort are needed to clarify the role of the connections with other important structures, such as the brainstem and basal ganglia. Finally, our work accounted only for structural connections of CM, whereas animal models of CM-DBS implementing DTI analysis with functional connections from fMRI data described a wider array of brain connectivity for this thalamic nucleus.[89] In fact, structural and functional connectivity profiles of the same anatomic area may not completely overlap, and fMRI activation may result from indirect structural connections between different brain regions.[90] Interestingly, a recent study demonstrated that epileptogenic post-stroke lesions were included in a brain network defined by functional connectivity with the cerebellum and the basal ganglia, and that VTAs from ANT-DBS patients were associated with the same functional network.[91] Therefore, further studies employing both structural and connectivity analysis are warranted to corroborate the results of our work.

Conclusion

Our study showed that the CM nucleus had stronger structural connectivity with the brainstem, the basal ganglia, the cerebellum and the primary sensorimotor and premotor areas, but weaker connectivity with structures traditionally classified as limbic. Since the sweet-spot demonstrated a higher probability of connectivity with frontal and prefrontal cortices, our analysis corroborated the beneficial effect of CM-neuromodulation for LGS patients, according to the cortically centered pathophysiology of this particular disease. Nevertheless, our results also suggested a promising role for the cerebellum, which might contribute to controlling generalized seizures by desynchronizing the whole brain via its widespread structural connections. That being said, generalized epilepsy is a complex disease and abnormal electrical activity in different brain

regions may underline a similar epileptic semeiology. The fact that stronger CM connections with the cerebellum in the HCP cohort were supported by the results of the same analysis in the patients' cohort led us to hypothesize that cerebellar activity via CM stimulation might halt seizures in generalized epilepsy. However, it is more realistic that cerebellar connections are one piece of a more complicated puzzle explaining the anti-seizure effect of CM-neuromodulation, and other connections may also exert a function for seizure control. In fact, several studies sustained that a personalized pattern of connections may benefit different patients according to their epilepsy subtypes and the choice of the surgical target for neuromodulation in generalized DRE should be tailored accordingly.[69,92] In this context, our study demonstrated that probabilistic tractography can be employed to identify the most significant CM connections, which can be specifically targeted during preoperative surgical planning as previously illustrated by DBS for movement disorders[93,94] and psychiatric conditions.[95,96] Moreover, understanding the connectivity of surgical targets used in neuromodulation procedures for the DRE treatment assumes further importance if considered in the context of closed-loop stimulation, which has been shown to increase the response to neurostimulation in Parkinson's disease[97] and depressed[98] patients and has also been proposed for epilepsy.[99] Therefore, our results contribute to laying the groundwork for refining the targeting of the CM nucleus in order to improve the clinical outcome after neuromodulation surgery in patients suffering from generalized DRE.

Declarations

Author contributions
Luigi G. Remore: Conceptualization; Data curation; Formal analysis; Investigation;

ORCID iD
Luigi G. Remore https://orcid.org/0000-0003-4118-9009

Supplemental material
Supplemental material for this article is available online.

References

1. Beghi E. The epidemiology of epilepsy. *Neuroepidemiology* 2020; 54: 185–191.
2. Atrick P, Wan K, Artin M, *et al.* Early identification of refractory epilepsy. *N Engl J Med* 2000; 342: 314–319.
3. Jobst BC and Cascino GD. Resective epilepsy surgery for drug-resistant focal epilepsy: a review. *JAMA* 2015; 313: 285–293.
4. Lin Y and Wang Y. Neurostimulation as a promising epilepsy therapy. *Epilepsia Open* 2017; 2: 371–387.
5. Fisher R, Salanova V, Witt T, *et al.* Electrical stimulation of the anterior nucleus of thalamus for treatment of refractory epilepsy. *Epilepsia* 2010; 51: 899–908.
6. Kaufmann E, Bartolomei F, Boon P, *et al.* European expert opinion on ANT-DBS therapy for patients with drug-resistant epilepsy (a Delphi consensus). *Seizure* 2020; 81: 201–209.
7. Kwon CS, Jetté N and Ghatan S. Perspectives on the current developments with neuromodulation for the treatment of epilepsy. *Expert Rev Neurother* 2020; 20: 189–194.
8. Zangiabadi N, Ladino LD, Sina F, *et al.* Deep brain stimulation and drug-resistant epilepsy: A review of the literature. *Front Neurol* 2019; 10: 601.
9. Ryvlin P, Rheims S, Hirsch LJ, *et al.* Neuromodulation in epilepsy: state-of-the-art approved therapies. *Lancet Neurol* 2021; 20: 1038–1047.
10. Velasco F, Velasco M, Ogarrio C, *et al. Electrical stimulation of the Centromedian thalamic nucleus in the treatment of convulsive seizures: a preliminary report. Epilepsia* 1987; 28: 421–430.
11. Vetkas A, Fomenko A, Germann J, *et al.* Deep brain stimulation targets in epilepsy: systematic review and meta-analysis of anterior and centromedian thalamic nuclei and hippocampus. *Epilepsia* 2022; 63: 513–524.

12. Beaudreault CP, Muh CR, Naftchi A, *et al.* Responsive neurostimulation targeting the anterior, centromedian and pulvinar thalamic nuclei and the detection of electrographic seizures in pediatric and Young Adult Patients. *Front Hum Neurosci* 2022; 16: 1–15.

13. Sisterson ND, Kokkinos V, Urban A, *et al.* Responsive neurostimulation of the thalamus improves seizure control in idiopathic generalised epilepsy: Initial case series. *J Neurol Neurosurg Psychiatry* 93: 491–498.

14. Kokkinos V, Urban A, Sisterson ND, *et al.* Responsive neurostimulation of the thalamus improves seizure control in idiopathic generalized epilepsy: a case report. *Neurosurg* 2020; 87: E578–E583.

15. Warsi NM, Yan H, Suresh H, *et al.* The anterior and centromedian thalamus: anatomy, function, and dysfunction in epilepsy. *Epilepsy Res* 2022; 182: 106913.

16. Ilyas A, Pizarro D, Romeo AK, *et al.* The centromedian nucleus: anatomy, physiology, and clinical implications. *J Clin Neurosci* 2019; 63: 1–7.

17. Benarroch EE. The midline and intralaminar thalamic nuclei Anatomic and functional specificity and implications in neurologic disease. *Neurology.* Epub ahead of print 15 September 2008.

18. Sadikot AF and Rymar VV. The primate centromedian-parafascicular complex: anatomical organization with a note on neuromodulation. *Brain Res Bull* 2009; 78: 122–130.

19. Velasco M, Velasco F, Velasco AL, *et al.* Acute and chronic electrical stimulation of the centromedian thalamic nucleus: modulation of reticulo-cortical systems and predictor factors for generalized seizure control. *Arch Med Res* 2000; 31: 304–315.

20. Warren AEL, Dalic LJ, Bulluss KJ, *et al.* The optimal target and connectivity for deep brain stimulation in Lennox-Gastaut syndrome. *Ann Neurol* 2022; 92: 61–74.

21. Dalic LJ, Warren AEL, Bulluss KJ, *et al.* DBS of thalamic centromedian nucleus for Lennox-Gastaut syndrome (ESTEL Trial). *Ann Neurol* 2022; 91: 253–267.

22. Krauth A, Blanc R, Poveda A, *et al.* A mean three-dimensional atlas of the human thalamus: generation from multiple histological data. *Neuroimage* 2010; 49: 2053–2062.

23. Glasser MF, Sotiropoulos SN, Wilson JA, *et al.* The minimal preprocessing pipelines for the Human Connectome Project. *Neuroimage* 2013; 80: 105–124.

24. Glasser MF, Smith SM, Marcus DS, *et al.* The human connectome project's neuroimaging approach. *Nat Neurosci* 2016; 19: 1175–1187.

25. Kwan P, Arzimanoglou A, Berg AT, *et al.* Definition of drug resistant epilepsy: consensus proposal by the ad hoc Task Force of the ILAE commission on therapeutic strategies. *Epilepsia* 2010; 51: 1069–1077.

26. Smith SM. Fast robust automated brain extraction. *Hum Brain Mapp* 2002; 17: 143–155.

27. Jenkinson M, Bannister P, Brady M, *et al.* Improved optimization for the robust and accurate linear registration and motion correction of brain images. *Neuroimage* 2002; 17: 825–841.

28. Behrens TE, Berg HJ, Jbabdi S, *et al.* Probabilistic diffusion tractography with multiple fibre orientations: What can we gain? *Neuroimage* 2007; 34: 144–155.

29. Behrens TE, Woolrich MW, Jenkinson M, *et al.* Characterization and propagation of uncertainty in diffusion-weighted MR Imaging. *Magn Reson Med* 2003; 50: 1077–1088.

30. Velasco AL, Velasco F, Jiménez F, *et al.* Neuromodulation of the centromedian thalamic nuclei in the treatment of generalized seizures and the improvement of the quality of life in patients with Lennox-Gastaut syndrome. *Epilepsia* 2006; 47: 1203–1212.

31. Velasco F, Velasco AL and Velasco M. Deep brain stimulation for treatment of the epilepsies: the centromedian thalamic target. In: Sakas DE and Simpson BA (eds) *Operative neuromodulation: volume 2: neural networks surgery.* Vienna: Springer, 2007, pp. 337–342.

32. Horn A, Reich M, Vorwerk J, *et al.* Connectivity predicts deep brain stimulation outcome in Parkinson disease. *Ann Neurol* 2017; 82: 67–78.

33. Elias GJB, Boutet A, Joel SE, *et al.* Probabilistic mapping of deep brain stimulation: insights from 15 Years of therapy. *Ann Neurol* 2021; 89: 426–443.

34. Loh A, Elias GJB, Germann J, *et al.* Neural correlates of optimal deep brain stimulation for cervical dystonia. *Ann Neurol* 2022; 92: 418–424.

35. Astrom M, Diczfalusy E, Martens H, *et al.* Relationship between neural activation and electric field distribution during deep brain stimulation. *IEEE Trans Biomed Eng* 2015; 62: 664–672.

36. Su JH, Thomas FT, Kasoff WS, *et al.* Thalamus optimized multi atlas segmentation (THOMAS): fast, fully automated segmentation of thalamic nuclei from structural MRI. *Neuroimage* 2019; 194: 272–282.

37. Alcala-Zermeno JL, Gregg NM, Wirrell EC, *et al.* Centromedian thalamic nucleus with or without anterior thalamic nucleus deep brain stimulation for epilepsy in children and adults: A retrospective case series. *Seizure* 2021; 84: 101–107.

38. Fischl B. FreeSurfer. *NeuroImage* 2012; 62: 774–781.

39. Tsolaki E, Espinoza R and Pouratian N. Using probabilistic tractography to target the subcallosal cingulate cortex in patients with treatment resistant depression. *Psychiatry Res Neuroimaging* 2017; 261: 72–74.

40. Tsolaki E, Sheth SA and Pouratian N. Variability of white matter anatomy in the subcallosal cingulate area. *Hum Brain Mapp* 2021; 42: 2005–2017.

41. Tsolaki E, Downes A, Speier W, *et al.* The potential value of probabilistic tractography-based for MR-guided focused ultrasound thalamotomy for essential tremor. *NeuroImage Clin* 2018; 17: 1019–1027.

42. Riskin-Jones HH, Kashanian A, Sparks H, *et al.* Increased structural connectivity of thalamic stimulation sites to motor cortex relates to tremor suppression. *NeuroImage Clin* 2021; 30: 102628.

43. Li W, Qin W, Liu H, *et al.* Subregions of the human superior frontal gyrus and their connections. *Neuroimage* 2013; 78: 46–58.

44. van der Werf YD, Witter MP and Groenewegen HJ. *The intralaminar and midline nuclei of the thalamus. Anatomical and functional evidence for participation in processes of arousal and awareness. Brain Res Brain Res Rev* 2002; 39: 107–140. (2002).

45. Weigel R and Krauss JK. Center median-parafascicular complex and pain control: review from a neurosurgical perspective. *Stereotact Funct Neurosurg* 2004; 82: 115–126.

46. Bohlhalter S, Goldfine A, Matteson S, *et al.* Neural correlates of tic generation in Tourette syndrome: an event-related functional MRI study. *Brain* 2006; 129: 2029–2037.

47. Jaggi AS and Singh N. Role of different brain areas in peripheral nerve injury-induced neuropathic pain. *Brain Res* 2011; 1381: 187–201.

48. Eskandar E, Chudy D, Deletis V, *et al.* Thalamic stimulation in vegetative or minimally conscious patients. *J Neurosurg* 2018; 128: 1187–1188.

49. Warren AEL, Dalic LJ, Thevathasan W., *et al* Targeting the centromedian thalamic nucleus for deep brain stimulation. *J Neurol Neurosurg Psychiatry* 2020; 91: 339–349.

50. Son BC, Shon YM, Choi JG, *et al.* Clinical outcome of patients with deep brain stimulation of the centromedian thalamic nucleus for refractory epilepsy and location of the active contacts. *Stereotact Funct Neurosurg* 2016; 94: 187–197.

51. Kros L, Eelkman Rooda OHJ, De Zeeuw CI, *et al.* Controlling cerebellar output to treat refractory epilepsy. *Trends Neurosci* 2015; 38: 787–799.

52. Meencke H-J. Neuron density in the molecular layer of the frontal cortex in primary generalized epilepsy. *Epilepsia* 1985; 26: 450–454.

53. O'Muircheartaigh J and Richardson MP. Epilepsy and the frontal lobes. *Cortex* 2012; 48: 144–155.

54. Klimpe S, Behrang-Nia M, Bott MC, *et al.* Recruitment of motor cortex inhibition differentiates between generalized and focal epilepsy. *Epilepsy Res* 2009; 84: 210–216.

55. Molnar GF, Sailer A, Gunraj CA, *et al.* Changes in motor cortex excitability with stimulation of anterior thalamus in epilepsy. *Neurology* 2006; 66: 566–571.

56. Miller KJ, Burns TC, Grant GA, *et al.* Responsive stimulation of motor cortex for medically and surgically refractive epilepsy. *Seizure* 2015; 33: 38–40.

57. Child ND, Stead M, Wirrell EC, *et al.* Chronic subthreshold subdural cortical stimulation for the treatment of focal epilepsy originating from eloquent cortex. *Epilepsia* 2014; 55: e18–e21.

58. Vulliemoz S, Vollmar C, Koepp MJ, *et al.* Connectivity of the supplementary motor area in juvenile myoclonic epilepsy and frontal lobe epilepsy. *Epilepsia* 2011; 52: 507–514.

59. Warren AEL, Harvey AS, Vogrin SJ, *et al.* The epileptic network of Lennox-Gastaut syndrome: cortically driven and reproducible across age. *Neurology* 2019; 93: E215–E226.

60. de la Vega A, Chang LJ, Banich MT, *et al.* Large-scale meta-analysis of human medial frontal cortex reveals tripartite functional organization. *ARC J Neurosci* 2016; 36: 6553–6562.

61. Chen Y, Landin-Romero R, Kumfor F, *et al.* Cerebellar structural connectivity and contributions to cognition in frontotemporal dementias. *Cortex* 2020; 129: 57–67.

62. Chen Z, Zhang R, Huo H, *et al.* Functional connectome of human cerebellum. *Neuroimage* 2022; 251: 119015.

63. McAfee SS, Liu Y, Sillitoe RV, *et al.* Cerebellar coordination of neuronal communication in Cerebral Cortex. *Front Syst Neurosci* 2022; 15: 781527.

64. Boop S, Wheless J, Van Poppel K, *et al.* Cerebellar seizures. *J Neurosurg Pediatr* 2013; 12: 288–292.

65. Lawson JA, Vogrin S, Bleasel AF, *et al.* Cerebral and cerebellar volume reduction in children with intractable epilepsy. *Epilepsia* 2000; 41: 1456–1462.

66. Marcián V, Mareček R, Koriťáková E, *et al.* Morphological changes of cerebellar substructures in temporal lobe epilepsy: a complex phenomenon, not mere atrophy. *Seizure* 2018; 54: 51–57.

67. Kros L, Eelkman Rooda OH, Spanke JK, *et al.* Cerebellar output controls generalized spike-and-wave discharge occurrence. *Ann Neurol* 2015; 77: 1027–1049.

68. Kay BP, Holland SK, Privitera MD, *et al.* Differences in paracingulate connectivity associated with epileptiform discharges and uncontrolled seizures in genetic generalized epilepsy. *Epilepsia* 2014; 55: 256–263.

69. Piper RJ, Richardson RM, Worrell G, *et al.* Towards network-guided neuromodulation for epilepsy. *Brain* 2022; 145: 3347–3362.

70. Velasco F, Carrillo-Ruiz JD, Brito F, *et al.* Double-blind, randomized controlled pilot study of bilateral cerebellar stimulation for treatment of intractable motor seizures. *Epilepsia* 2005; 46: 1071–1081.

71. Van Buren JM, Wood JH, Oakley J, *et al.* Preliminary evaluation of cerebellar stimulation by double-blind stimulation and biological criteria in the treatment of epilepsy. *J Neurosurg* 1978; 48: 407–416.

72. Cooper IS, Amin I, Riklan M, *et al.* Chronic cerebellar stimulation in epilepsy. Clinical and anatomical studies. *Arch Neurol* 1976; 33: 559–570.

73. Voogd J. The human cerebellum. *J Chem Neuroanat* 2003; 26: 243–252.

74. Eelkman Rooda OHJ, Kros L, Faneyte SJ, *et al.* Single-pulse stimulation of cerebellar nuclei stops epileptic thalamic activity. *Brain Stimul* 2021; 14: 861–872.

75. Rondi-Reig L. The cerebellum on the epilepsy frontline. *Trends Neurosci* 2022; 45: 337–338.

76. Jiang S, Li X, Li Z, *et al.* Cerebello-cerebral connectivity in idiopathic generalized epilepsy. *Eur Radiol* 2020; 30: 3924–3933.

77. Streng ML and Krook-Magnuson E. The cerebellum and epilepsy. *Epilepsy Behav* 2021; 121: 106909.

78. Hunter J and Jasper HH. Effects of thalamic stimulation in unanaesthetised animals. The arrest reaction and petit mal-like seizures, activation patterns and generalized convulsions. *Electroencephalogr Clin Neurophysiol* 1949; 1: 305–324.

79. Carney PW, Masterton RA, Harvey AS, *et al.* The core network in absence epilepsy: differences in cortical and thalamic BOLD response. *Neurology* 2010; 75: 904–911.

80. Ren L, Yu T, Wang D, *et al.* Subthalamic nucleus stimulation modulates motor epileptic activity in humans. *Ann Neurol* 2020; 88: 283–296.

81. Soper C, Wicker E, Kulick CV, *et al.* Optogenetic activation of superior colliculus neurons suppresses seizures originating in diverse brain networks. *Neurobiol Dis* 2016; 87: 102–115.

82. Kundishora AJ, Gummadavelli A, Ma C, *et al.* Restoring conscious arousal during focal limbic seizures with deep brain stimulation. *Cereb Cortex* 2017; 27: 1964–1975.

83. Torres Diaz CV, González-Escamilla G, Ciolac D, *et al.* Network substrates of centromedian nucleus deep brain stimulation in generalized pharmacoresistant epilepsy. *Neurother* 2021; 18: 1665–1677.

84. Masterton RA, Carney PW, Abbott DF, *et al.* Absence epilepsy subnetworks revealed by event-related independent components analysis of functional magnetic resonance imaging. *Epilepsia* 2013; 54: 801–808.

85. Dalic LJ, Warren AEL, Young JC, *et al.* Cortex leads the thalamic centromedian nucleus in generalized epileptic discharges in Lennox-Gastaut syndrome. *Epilepsia* 2020; 61: 2214–2223.

86. Remore LG, Omidbeigi M, Tsolaki E, *et al.* Deep brain stimulation of thalamic nuclei for the treatment of drug-resistant epilepsy: are we

confident with the precise surgical target? *Seizure* 2023; 105: 22–28.

87. Maier-Hein KH, Neher PF and Houde JC. The challenge of mapping the human connectome based on diffusion tractography. *Nat Commun.* Epub ahead of print 1 December 2017.

88. Tournier JD, Mori S and Leemans A. Diffusion tensor imaging and beyond. *Magn Reson Med* 2011; 65: 1532–1556.

89. Kim JP, Min HK, Knight EJ, *et al.* Centromedian-parafascicular deep brain stimulation induces differential functional inhibition of the motor, associative, and limbic circuits in large animals. *Biol Psychiatry* 2013; 74: 917–926.

90. Damoiseaux JS and Greicius MD. Greater than the sum of its parts: a review of studies combining structural connectivity and resting-state functional connectivity. *Brain Struct Funct* 2009; 213: 525–533.

91. Schaper FLWVJ, Nordberg J, Cohen AL, *et al.* Mapping lesion-related epilepsy to a Human Brain Network. *JAMA Neurol* 2023; 80: 891–902.

92. Sisterson ND and Kokkinos V. Neuromodulation of epilepsy networks. *Neurosurg Clin N Am* 2020; 31: 459–470.

93. Petersen MV, Lund TE, Sunde N, *et al.* Probabilistic versus deterministic tractography for delineation of the cortico-subthalamic hyperdirect pathway in patients with Parkinson disease selected for deep brain stimulation. *J Neurosurg* 2017; 126: 1657–1668.

94. Fenoy AJ and Schiess MC. Comparison of tractography-assisted to atlas-based targeting for deep brain stimulation in essential tremor. *Mov Disord* 2018; 33: 1895–1901.

95. Riva-Posse P, Choi KS, Holtzheimer PE, *et al.* A connectomic approach for subcallosal cingulate deep brain stimulation surgery: prospective targeting in treatment-resistant depression. *Mol Psychiatry* 2018; 23: 843–849.

96. Coenen VA, Sajonz B, Reisert M, *et al.* Tractography-assisted deep brain stimulation of the superolateral branch of the medial forebrain bundle (slMFB DBS) in major depression. *NeuroImage Clin* 2018; 20: 580–593.

97. Bouthour W, Mégevand P, Donoghue J, *et al.* Biomarkers for closed-loop deep brain stimulation in Parkinson disease and beyond. *Nat Rev Neurol* 2019; 15: 343–352.

98. Scangos KW, Khambhati AN, Daly PM, *et al.* Closed-loop neuromodulation in an individual with treatment-resistant depression. *Nat Med* 2021; 27: 1696–1700.

99. Kokkinos V, Sisterson ND, Wozny TA, *et al.* Association of closed-loop brain stimulation neurophysiological features with seizure control among patients with focal epilepsy. *JAMA Neurol* 2019; 76: 800–808.

Visit Sage journals online journals.sagepub.com/home/tan

§ Sage journals